

# Transient Evaluation of Grounding Encased in Concrete: a Study Based on Real Measurements in Power Systems Configurations

Alex B. Tronchoni, Daniel Gazzana, Guilherme A. D. Dias, Roberto C. Leborgne, Arturo S. Bretas, Marcos Telló

**Abstract--** This paper presents a study in order to evaluate the performance of grounding systems embedded in concrete (UFER). The main topologies used in transmission and distribution network as rod, mesh, cross and T were considered. The study was carried out for soils with low and high resistivity. Important aspects regarding to the measurement process, surge generator prototype and a pilot project implemented in a 69 kV transmission line are also reported. The measurement experiments showed a means reduction for both surge impedance and static resistance above 53 % considering the use of UFER for a soil with 293  $\Omega\text{m}$ . Finally, a static resistance reduction ranging from 62 % to 93 % was observed to soil with high resistivity, above 1000  $\Omega\text{m}$ .

**Keywords:** Grounding encased in concrete, lightning, surge generator, real measurements, UFER.

## I. INTRODUCTION

**B**OTH in transmission lines (TL) and distribution networks, the electric power utilities have as one of the reasons of consumer disconnections the inadequate working of the associated grounding system. In most cases, the grounding is designed to work effectively against short-circuit faults related to low frequency (60 Hz) in steady state. In the case of transient phenomena associated with high frequencies (MHz), as in the occurrence of a lightning or even in an equipment switching, such grounding usually presents inadequate performance. Especially in the case of TLs, its shielding is strongly affected by the efficiency of the grounding system, mainly in the process to dissipate to the earth a surge that reaches directly or indirectly an overhead conductor.

An especial concern should be highlighted in areas where the soil presents high values of resistivity. In this condition is difficult, if not impossible, to obtain low grounding impedance

---

This work was supported in part by FAPERGS, CAPES, CNPQ, Ministry of Education of Brazil and Companhia Estadual de Energia Elétrica – CEEE-D. Alex B. Tronchoni, Daniel Gazzana, Guilherme A. D. Dias and Roberto C. Leborgne are with Federal University of Rio Grande do Sul - UFRGS, Porto Alegre, RS 90035-190, Brazil, (e-mail: alex.tronchoni@ufrgs.br; dgazzana@ece.ufrgs.br, gaddias@terra.com.br; rcl@ece.ufrgs.br). Arturo S. Bretas is with University of Florida, Gainesville, FL 32611, USA and Federal University of Rio Grande do Sul - UFRGS, Porto Alegre, RS 90035-190, Brazil, (e-mail: arturo@ece.ufl.edu, abretas@ece.ufrgs.br). Marcos Telló is with Companhia Estadual de Energia Elétrica – CEEE-D, Porto Alegre, RS 91410-400, Brazil, (e-mail: marcost@ceee.com.br).

Paper submitted to the International Conference on Power Systems Transients (IPST2017) in Seoul, Republic of Korea June 26-29, 2017

values, which lead to better efficiency of the lightning protection system (LPS).

Over the past years various methods and techniques have been developed to improve the performance of LPS. One of these methods is to encase the grounding system in concrete, also called UFER grounding [1].

The low electric resistance obtained from the cement and its ability to absorb moisture are some of the characteristics of this material, which should be used as a component of the grounding system enabling its application in the LPS to withstand lightning impulses [2].

One of the shortcomings related the use of the grounding embedded in concrete is the lack of knowledge about the performance and behavior of this grounding system type regarding to the reduction of the voltages and impedance on the electrode.

In this context, the goal of this paper is to present a study based on field measurements of the main grounding topologies used in transmission and distribution networks (rod, mesh, cross and T). In order to provide qualitative knowledge about their efficiency, these structures were subjected to surge impulses with and without grounding embedded in concrete. The study took into consideration soils with low resistivity around 300  $\Omega\text{m}$ , as well as soils with high resistivity ranging from 1054  $\Omega\text{m}$  to 2180  $\Omega\text{m}$ .

## II. GROUNDING ANALYSIS BACKGROUND

### A. Surge Impedance and Static Resistance.

The surge impedance  $Z$  is essential for determining the performance of grounding systems while current flows to the earth, as in the case of lightning discharges and transient faults.

Different definitions for surge impedance can be found in the literature [3]-[5]. The best choice is subjected to the characteristics of the problem in analysis. For this reason, the adopted formulation defined in [5] was used to calculate the surge impedance (1),

$$Z = \frac{\max[v(t)]}{I} \quad (\Omega) \quad (1)$$

where:  $Z$  is the surge impedance,  $I$  is the current value when  $v(t)$  is maximal.

The static resistance  $R$  is the value which the transient impedance curve  $z(t)$  converges in the end of the transitory period. In other words,  $R$  is the resistance in steady state and can be estimated numerically based on the discrete solution of

the Duhamel Integral Equation.

### B. Duhamel Integral Equation

The Duhamel Integral [6] is a way of calculating the response of linear systems to external perturbations in time-domain. So, the output  $v(t)$  of a linear circuit subjected to an arbitrary impulse can be calculated using (2) [7],

$$v(t) = i(0) \cdot z(t) + \int_0^t z(t-\tau) i'(\tau) d\tau \quad (\text{V}) \quad (2)$$

where:  $z(t)$  is the transient impedance in instant  $t$  and  $i(0)$  is the current in the circuit at time instant equal to zero.

Using  $v(t)$  and  $i(t)$ , which are known from the measurements, it is possible to determine  $z(t)$  utilizing the discrete form of Duhamel Integral (3), where the variables subscribe refers to the instants of time.

$$\begin{cases} i_1 = v_1 = 0 & (\text{A,V}) \\ z_1 = \frac{v_2}{i_2} & (\Omega) \\ z_n = \frac{1}{i_2} \cdot \left[ v_{n+1} - \sum_{m=2}^n z_{n-m+1} \cdot (i_{m+1} - i_m) \right], n = 2..N & (\Omega) \end{cases} \quad (3)$$

### C. Voltage Impulse Generator Prototype

Fig. 1 and Fig. 2 show the impulse generator prototype constructed for the experiments and the voltage impulse generator circuit diagram, respectively.



Fig. 1. Voltage impulse generator prototype.

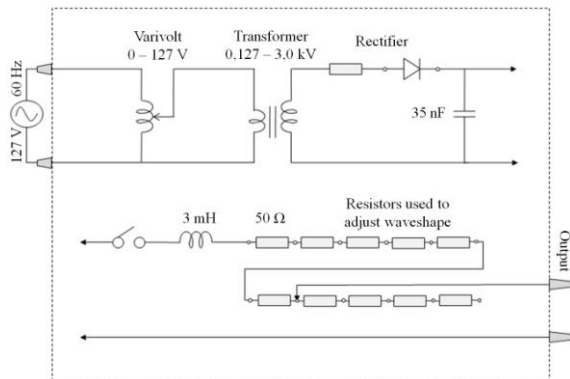


Fig. 2. Voltage impulse generator circuit diagram.

## III. EVALUATED GROUNDING TOPOLOGIES

The measurements were carried out for four types of grounding topologies with and without concrete: rod, mesh, cross and T. The small lightning symbol in each topology presented in Fig. 3 to Fig. 6 indicates the position in the structure where the impulse was injected.

The voltage impulse characterized by a double exponential function presented in (4)  $V_p$  (32 x 233)  $\mu\text{s}$  was used to represent the lightning surge,

$$v(t) = V_p \cdot (e^{-\alpha t} - e^{-\beta t}) \quad (\text{V}) \quad (4)$$

where:  $v(t)$  is the voltage impulse (V);  $V_p$  is the peak voltage (V);  $\alpha$  and  $\beta$  are time constants associated with front-time (32  $\mu\text{s}$ ) and half-time (233  $\mu\text{s}$ ) values. The following topologies were considered in the measurements:

Topology 1: rod with 2.4 m length, buried at 0.5 m depth and conductor diameter equal to 15.8 mm (5/8"). A side view of the grounding rod is shown in Fig. 3.

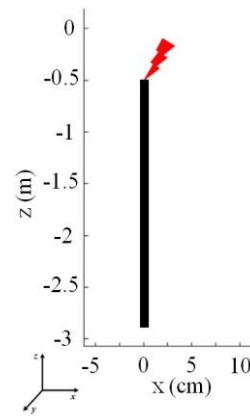


Fig. 3. Side view of the grounding rod.

Topology 2: 1.4 m x 1.4 m square grounding mesh with 11 by 11 electrodes 0.14 m x 0.14 m, buried at 0.5 m depth with 4 rods in the corners as described in topology 1. The mesh was constructed with 6 AWG (4.11 mm) copper wire. Fig. 4 depicts the top view of the grounding mesh.

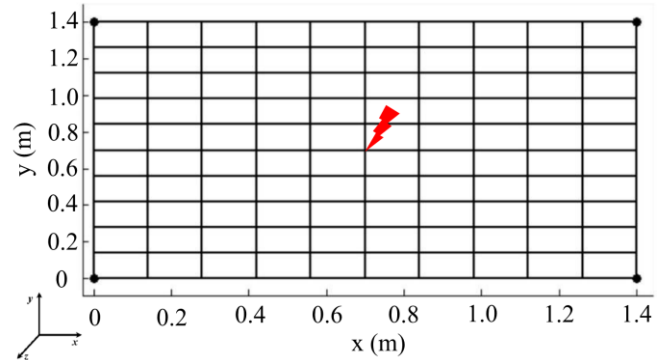


Fig. 4. Top view of the grounding mesh topology. Black dots at the corners represent rods.

Topology 3: cross grounding, buried at 0.5 m depth, constructed with 6 AWG (4.11 mm) copper wire connecting 13 rods, 3 at each direction and one at the center spaced in 2.9 m. Fig. 5 shows the top view of the cross grounding.

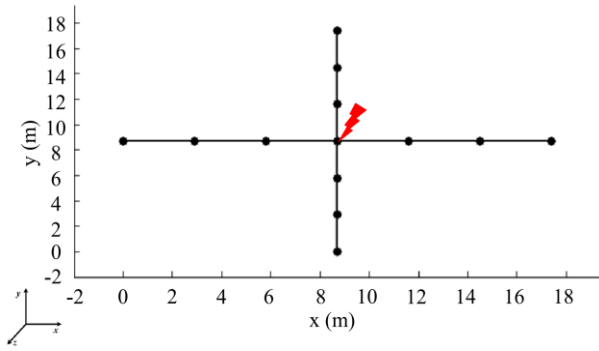


Fig. 5. Top view of the cross grounding topology. Black dots represent rods.

Topology 4: T grounding, buried at 0.5 m depth, constructed with 6 AWG (4.11 mm) copper wire connecting 13 rods, 4 at each direction and one at the center spaced in 2.9 m. In Fig. 6 the top view of the T grounding is illustrated.

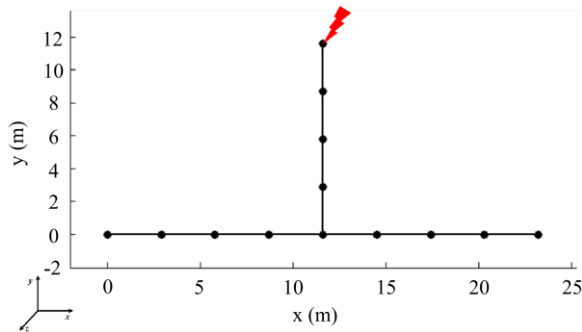


Fig. 6. Top view of the T grounding topology. Black dots represent rods.

#### IV. MEASUREMENTS

In the following is presented a description of the procedures to record transient voltages and currents in the studied grounding topologies. Before taking place the experiments it is important to determine the soil resistivity, since that the value of this electrical quantity may have an impact in the transient impedance analysis [8]. The Wenner Four-Electrode method [9] was used for this purpose and the measured soil resistivity stratified in one layer was determined as 293  $\Omega\text{m}$ .

The equipment used to perform the field measurements are presented below:

- Voltage impulse generator prototype;
- Tektronix DPO2014B digital oscilloscope (4 channel, bandwidth DC - 100 MHz);
- Tektronix TCP0150 current probe (bandwidth DC - 20 MHz);
- Tektronix P6015A passive high voltage probe (bandwidth DC - 75 MHz);
- Copper cables;
- 4 terminal ground resistance tester;
- Laptop.

Voltages and currents measurements and data acquisition were carried out using a special circuit setup, as illustrated in Fig. 7 and in accordance with [10]. It includes the impulse generator, the oscilloscope connected to the voltage and current probes, a voltage and a current electrode buried in the soil and the electrode under test (grounding structure). Data

was transferred from the oscilloscope to the laptop using an USB cable and a dedicated Tektronix communication protocol.

The measurement procedure for UFER grounding is the same as for conventional grounding. The only difference is that in UFER structures the electrode under test was embedded in concrete.

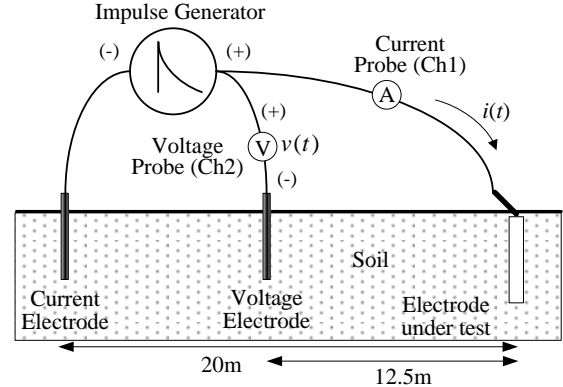


Fig. 7. Circuit setup used for the measurements. Adapted from [10].

#### V. RESULTS

This section presents the measurements results considering conventional grounding and UFER, aiming to evaluate the effect in surge impedance and static resistance when an impulse voltage is injected in different grounding systems using electrodes under test encased in concrete. In order to guarantee the consistency of results, the measurements were repeated three times, for each grounding topology, with and without concrete.

The recorded raw data in the field measurements presented a degree of noise and could lead to a wrong data analysis. For this reason, a smoothing function from Matlab called "*smooth*" was applied for voltage and current vectors. The function works as follows,  $Z = \text{smooth}(Y, \text{SPAN})$  smooths data  $Y$  (voltage or current) using  $\text{SPAN}$  (equal to 60) as the number of points used to compute each element of  $Z$ .

Fig. 8 and Fig. 9 demonstrates, respectively, the measured voltages and currents for conventional grounding rod and UFER grounding rod.

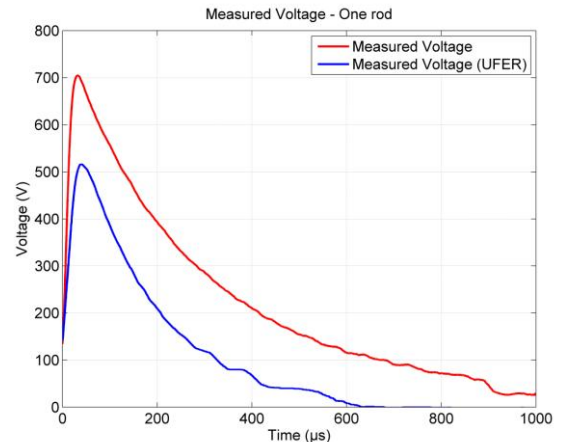


Fig. 8. Measured voltages for conventional grounding and UFER grounding.

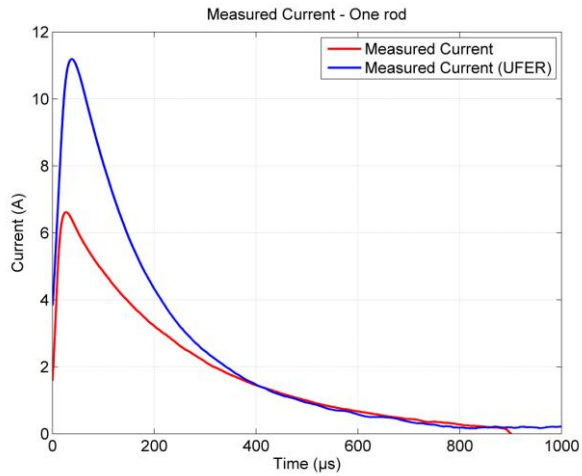


Fig. 9. Measured currents for conventional grounding and UFER grounding.

The transient impedance  $z(t)$  can be solved by using the discrete form of the Duhamel Integral, already mentioned in Section II - B. Fig. 10 shows the transient impedance  $z(t)$ , and the static resistance  $R$ , for grounding topologies with and without concrete.

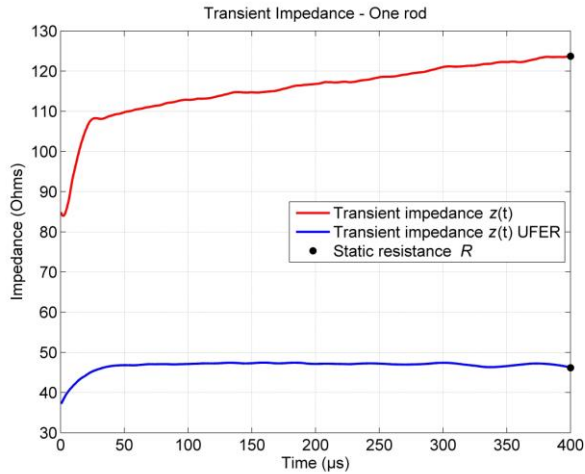


Fig. 10. Transient impedance  $z(t)$  and static resistance  $R$  for conventional grounding and UFER grounding.

Fig. 11 presents a bar chart showing the reduction in the static resistance  $R$  to the evaluated topologies based on the use of UFER. As result, the mean static resistance percent reduction equal to 54.64 % for a soil with resistivity of 293  $\Omega\text{m}$  was obtained.

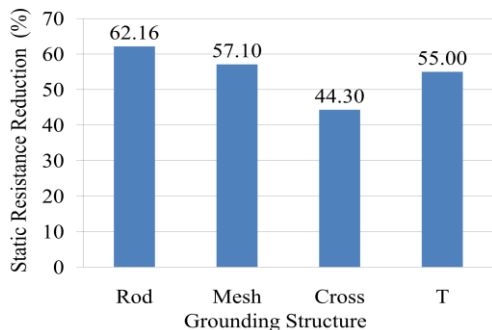


Fig. 11. Static resistance reduction for grounding systems embedded in concrete.

Table I also summarizes the experimental results. As can be seen, the current  $i(t)$  increases in the grounding topologies encased in concrete. Excepting for cross topology, a decrease in the electrodes potential  $v(t)$  is observed when UFER is used. For all configuration, there is a reduction in the surge impedance  $Z$ . The surge impedance mean percent reduction for a soil with 293  $\Omega\text{m}$  considering UFER was 53.74 %. As observed in the experiments, grounding encased in concrete leads to significant reduction in the surge impedance not only for soils with high resistivity, but also for soils with low resistivity [11]-[12].

TABLE I  
COMPARISON BETWEEN CONVENTIONAL GROUNDING AND GROUNDING ENCASED IN CONCRETE (UFER)

Grounding Topology	Experimental Results			
	$\max[v(t)]$ (V)	$I$ (A)	$z(t)$ ( $\Omega$ )	$z(t)$ Reduction (%)
Rod	704.57	6.57	107.16	56.92
Rod (UFER)	516.61	11.20	46.16	
Mesh	686.61	6.71	102.32	54.91
Mesh (UFER)	489.15	10.60	46.13	
Cross	405.93	3.04	133.64	49.77
Cross (UFER)	507.45	7.56	67.12	
T	630.67	3.50	180.45	53.37
T (UFER)	509.83	6.06	84.14	
Mean	-	-	-	53.74

## VI. PILOT PROJECT: GROUNDING ENCASED IN CONCRETE IN A 69 kV TRANSMISSION LINE

As commented previously, inadequate grounding systems are one of the main forced outage causes in TLLs.

In this way, a pilot project was implemented in a 69 kV TL in order to evaluate the performance of electrodes encased in concrete. The objective was to develop a methodology for the evaluation and design of grounding systems, giving emphasis to the soil, concrete and conductor arrangement considering high and low frequencies. The methodology was applied in a TL considering five different structure. Fig. 12 shows one of the grounding structures encased in concrete constructed for the pilot project. It consists of a trench approximately 1 m wide and 0.5 m deep.



Fig. 12. TL grounding structure encased in concrete.

In the following, the procedure to install a counterweight grounding in the transmission lines is presented.

1. Place the grounding conductor inside a trench;
2. Pour a thin layer of cement and then cover the conductor;
3. Let the cement cover about 30 cm of the conductor insulation;
4. Cover with approximately 10 cm of firmly compacted soil;
5. The trench must then be backfilled with earth and tamped.

The approximate dimensions of the electrode are as shown in Fig. 13. The length L (m) depends on the design of the transmission line counterweight. The height H and the width W are approximately 15 cm and 50 cm, respectively.

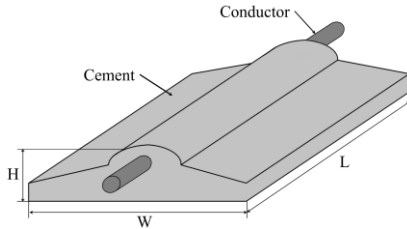


Fig. 13. Dimensions of the encased electrode.

Table II presents the results obtained before and after the utilization of the grounding encased in concrete. Five structures were evaluated. The measured soil resistivities at the areas where the experiment was performed ranges from 1054  $\Omega\text{m}$  to 2180  $\Omega\text{m}$ . The grounding static resistance before and after using UFER can be observed. The last column shows the static resistance percent reduction, varying from 62.77 % to 93.52 % and presenting a mean percent reduction of 84.84 %.

TABLE II  
COMPARISON BETWEEN STATIC RESISTANCE BEFORE AND AFTER USING  
GROUNDING ENCASED IN CONCRETE IN THE TRANSMISSION LINE

Structure ID of the TL	$\rho$ ( $\Omega\text{m}$ )	Static Resistance ( $\Omega$ )		Static Resistance Reduction (%)
		Before	After	
227	1054	98.6	36.7	62.77
226	1121	144	25	82.63
225	2080	190	28.3	85.10
224	2180	201	13.01	93.52
223	1630	132	13.02	90.13
Mean	1607.6	153.12	23.21	84.84

## VII. CONCLUSIONS

In this work, an evaluation of different grounding configurations (rod, mesh, cross and T) found in transmission and distribution network was presented. The focus of the study was concentrated in the analysis of the surge impedance and static resistance reductions in grounding systems when they are embedded in concrete.

The measurements showed a mean reduction of 54.64% for

the static resistance and a mean reduction of 53.74% for the grounding surge impedance considering soil with resistivity around 300  $\Omega\text{m}$ . Thus, in the performed experiments even in soils with low resistivity, the use of grounding encapsulated in concrete leads to a significant reduction of the involved quantities.

The encapsulated grounding was also implanted in a 69 kV TL, where five structures were encased in concrete resulting in a mean reduction of 85% in the grounding static resistance for soils with resistivity ranges from 1054  $\Omega\text{m}$  to 2080  $\Omega\text{m}$ .

Finally, this technique can be considered an efficient alternative to improve the grounding performance and consequently to reduce the outages in transmission lines and distribution networks.

## VIII. REFERENCES

- [1] T. L. Baldwin, R. Rifaat, and S. M. Malik, "Concrete encapsulated electrodes," in *Conference Record 2009 IEEE Industrial & Commercial Power Systems Technical Conference*, 2009, May, pp. 1–3.
- [2] C. L. Hallmark, "The use of Conductive Cement to Extend and Protect Made Ground Electrodes," in *AREMA Proceedings of the 2000 Annual Conference*, 2000.
- [3] C. F. Wagner and A. R. Hileman, "A New Approach to the Calculation or the Lightning Performance of Transmission Lines III-A Simplified Method: Stroke to Tower," *Transactions of the American Institute of Electrical Engineers. Part III: Power Apparatus and Systems*, vol. 79, no. 3, pp. 589–603, Apr. 1960.
- [4] F. P. Dawalibi, W. Ruan, S. Fortin, J. Ma and W. K. Daily, "Computation of power line structure surge impedances using the electromagnetic field method," *2001 IEEE/PES Transmission and Distribution Conference and Exposition. Developing New Perspectives (Cat. No.01CH37294)*, Atlanta, GA, 2001, pp. 663-668 vol.2.
- [5] H. Motoyama and H. Matsubara, "Analytical and experimental study on surge response of transmission tower," *IEEE Transactions on Power Delivery*, vol. 15, no. 2, pp. 812–819, Apr. 2000.
- [6] N. V. Korovkin, M. Hayakawa, S. L. Shishigin, Y. N. Bocharov, and S. Krivosheev, "Modeling of the grounded electrodes of power transmission towers," in *Book of abstracts EUROEM*, 2008, p. 234.
- [7] A. Smorgonskiy, N. Mora, F. Rachidi, M. Rubinstein, K. Sheshyekani, and N. Korovkin, "Measurements of transient grounding impedance of a wind turbine at the Mont-Crosin wind park," in *2015 Asia-Pacific Symposium on Electromagnetic Compatibility (APEMC)*, 2015, pp. 424–427.
- [8] R. Velazquez and D. Mukhedkar, "Analytical Modeling of Grounding Electrodes Transient Behavior," *IEEE Power Engineering Review*, vol. PER-4, no. 6, pp. 43–44, Jun. 1984.
- [9] *IEEE Guide for Measuring Earth Resistivity, Ground Impedance, and Earth Surface Potentials of a Grounding System*, IEEE Std 81-2012 (Revision of IEEE Std 81-1983), Dec. 2012
- [10] F. A. A. Souza, T. R. Neto, F. R. P. Magalhaes, F. B. Silva, and R. S. Pontes, "Predicting the Grounding Topology Based on Grounding Impedance and the Pattern Recognition Framework: A case study on one to four ground rods in straight line," *IEEE Transactions on Power Delivery*, 2016, (in press).
- [11] A. B. Tronchoni, D. S. Gazzana, G. A. D. Dias, R. C. Leborgne, A. S. Bretas, and M. Telló, "Impulsive Grounding Systems Embedded in Concrete: Theoretical and Practical Experiments," in *51st International Universities Power Engineering Conference*, 2016.
- [12] R. J. Cabral, D. S. Gazzana, A. B. Tronchoni, G. A. D. Dias, R. C. Leborgne, A. S. Bretas, and M. Telló, "Comparative performance of impulsive grounding systems embedded in concrete: An experiment in reduced scale," in *2016 33rd International Conference on Lightning Protection (ICLP)*, 2016.